

# Towards Quantum Simulation of Non-Markovian Open Quantum Dynamics: A Universal and Compact Theory

Xiang Li,<sup>1,\*</sup> Su-Xiang Lyu,<sup>1,\*</sup> Yao Wang,<sup>1,†</sup> Rui-Xue Xu,<sup>1</sup> Xiao Zheng,<sup>2,‡</sup> and YiJing Yan<sup>3,§</sup>

<sup>1</sup>Hefei National Research Center for Interdisciplinary Sciences at the Microscale,  
University of Science and Technology of China, Hefei, Anhui 230026, P. R. China

<sup>2</sup>Department of Chemistry, Fudan University, Shanghai 200433, P. R. China

<sup>3</sup>Hefei National Research Center for Interdisciplinary Sciences at the Microscale & iChEM,  
University of Science and Technology of China, Hefei, Anhui 230026, P. R. China

(Dated: February 12, 2024)

Non-Markovianity, the intricate dependence of an open quantum system on its temporal evolution history, holds tremendous implications across various scientific disciplines. However, accurately characterizing the complex non-Markovian effects has posed a formidable challenge for numerical simulations. Despite the promising potential of emerging quantum computing technologies, the pursuit of a universal theory enabling practical implementation of quantum computation algorithms remains ongoing. In this paper, we present a major advancement in bridging this critical gap: the development of dissipaton-embedded quantum master equation in second quantization (DQME-SQ). The DQME-SQ is an exact and compact theory, and its unique capabilities are demonstrated through digital quantum simulations of non-Markovian dissipative dynamics in both bosonic and fermionic environments. Our new theoretical developments pave the way for efficient exploration of complex open quantum systems.

*Introduction.* The simulation of open quantum systems (OQS) has attracted wide attention, because their interactions with the surrounding environment lead to intricate dynamical behavior [1–3]. OQS often exhibit non-Markovian features, characterized by memory effects where past states influence the current state. Understanding and characterizing non-Markovian effects are crucial for various physical processes such as quantum transport, quantum dephasing, coherent energy transfer, and precise measurement and control of quantum states [4–8]. For example, in biomolecular systems such as the Fenna-Matthews-Olson complex and the B800-850 ring, the non-Markovianity facilitates highly efficient energy conversion and charge transfer [9–12]. In strongly correlated quantum dots, non-Markovian memory leads to memristive behavior that may be harnessed in novel quantum device applications [6]. However, characterizing non-Markovian effect in OQS has remained a longstanding challenge.

Among the numerous attempts [13–28] to address this challenge, a representative method, the hierarchical equations of motion (HEOM) method [14], has gained significant attention. The HEOM method characterizes non-Markovianity through a two-time correlation function in the form of a memory kernel, which is decomposed and reorganized within a hierarchy to account for all the possible dissipation modes. However, the exponential growth of dynamical variables presents serious challenges in computational time and data storage, making it difficult to apply HEOM and other non-Markovian quantum dissipation methods to complex OQS within existing classical computational frameworks [14].

In recent years, the rapid progress in quantum technologies has launched a new era of computational ca-

capabilities, enabling exploration of previously inaccessible realms of the modern science [29–38]. Quantum computation holds promise for efficiently simulating OQS. Several quantum computing algorithms have been developed for simulating quantum dynamics [34, 35, 39–46], including full quantum algorithms [47–49] and quantum-classical hybrid algorithms based on the variational principle [50–53]. However, simulating non-Markovian OQS in quantum circuits remains a challenging task. In the HEOM method, the main difficulty lies in the complex structure of the coupled equations, leading to intricate quantum circuits representing the propagator.

This paper aims to establish a universal and compact theory, the dissipaton-embedded quantum master equation in second quantization (DQME-SQ), which enables the quantum simulation of non-Markovian open quantum dynamics.

*Construction of DQME-SQ theory.* In our previous work [54], we had established the dissipaton-embedded quantum master equation (DQME). This theory effectively decomposes the non-Markovian environment into a set of statistically independent generalized Brownian quasi-particles, referred to as *dissipatons* [55]. Depicted in Fig. 1(a) is the total composite system, consisting of the system of primary interest and its non-Markovian environment. In Fig. 1(b), the environment is represented by a series of dissipatons (red plates). The system interacts with these dissipatons, with each dissipaton carrying non-Markovian memory information through its characteristic energy and lifetime. The dissipaton behaves like a Brownian particle embedded in a Markovian bath (light blue dots). The dynamics of the extended system, consisting of the system and dissipatons, is governed by the DQME, which is a time-local Fokker-Planck-like equation

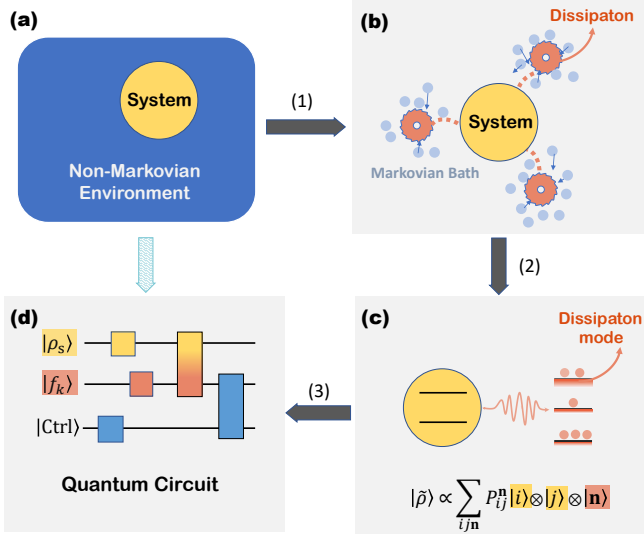


FIG. 1. Schematic representation of DQME-SQ theory for quantum simulation. Arrow (1) from panel (a) to (b) represents the mapping from the original environment to the individual dissipatons, statistically independent Brownian quasi-particles. In panel (c), dissipatons are second-quantized, represented by the creation and annihilation operators acting on the Fock states. Panel (d) sketches a quantum circuit that processes the qubit states encoding the dissipatons, with  $|Ctrl\rangle$  being an ancillary control bit for time propagation. As a result, the DQME-SQ enables quantum simulation of non-Markovian open quantum dynamics.

[54]. Taking the bosonic open quantum system as the example, the temporal evolution of density distribution of the extended system,  $\rho(x_1, x_2, \dots)$ , is governed by the DQME, where  $x_1, x_2, \dots$  are the coordinates of dissipatons. However, since the coordinates  $\{x_k\}$  are *continuous* variables, it is difficult to encode the DQME for quantum simulation purposes.

To overcome this difficulty, we notice that the quantum dissipation process can be fully characterized by a combination of generation and annihilation events of dissipatons. Such characterization corresponds to a second quantization procedure. In Fig. 1(c), each level corresponds to a dissipaton mode capable of accommodating multiple dissipatons. A dissipaton configuration is established by specifying the occupation numbers of all dissipaton modes. After applying the application of second quantization, the DQME-SQ governs the transitions between different Fock states of dissipatons. In principle, the non-Markovianity is exactly accounted for if all the possible dissipaton configurations are explicitly included in the open quantum dynamics. This is analogous to the electronic structure theory where full configuration interaction treatment yields exact many-body wavefunction.

The construction of DQME-SQ theory will first be exemplified with bosonic open quantum system. We always set  $\hbar = 1$  and  $\beta \equiv 1/(k_B T)$ , where  $k_B$  is the

Boltzmann constant and  $T$  the environment temperature. The total Hamiltonian has the generic form of  $H_T = H_S + H_E + H_{SE}$ . Here,  $H_S$  and  $H_E$  are the system and environment Hamiltonian, respectively. For brevity, the system-environment coupling is set as  $H_{SE} = \hat{Q}\hat{F}$ , where  $\hat{Q}$  is the system operator, and the environment operator  $\hat{F}$  incorporates the system-environment coupling strength. The non-Markovian memory of a Gaussian environment is fully characterized by the hybridization correlation function,  $C(t) = \langle \hat{F}(t)\hat{F}(0) \rangle_E$ . Here,  $\hat{F}(t) \equiv e^{iH_E t} \hat{F} e^{-iH_E t}$  and  $\langle \hat{O} \rangle_E \equiv \text{Tr}_E[\hat{O}e^{-\beta H_E}]/\text{Tr}_E(e^{-\beta H_E})$  is the ensemble average at the equilibrium state of bare environment, where  $\hat{O}$  is an arbitrary operator.

The DQME-SQ formalism starts with the dissipaton decomposition (DD) [cf. Arrow(1) in Fig. 1], which should preserve the correlation function  $C(t)$ . The DD maps the environment hybridization operator  $\hat{F}$  onto  $\{\hat{f}_k\}$ , the coordinate operators of dissipatons [55],

$$\hat{F} \xrightarrow{\text{DD}} \sum_{k=1}^K \hat{f}_k. \quad (1)$$

For individual dissipatons, we set  $\langle \hat{f}_k(t)\hat{f}_{k'}(0) \rangle_D = \delta_{kk'} c_k(t)$ , such that the non-Markovian memory of the original bosonic environment is fully recovered through the statistics of dissipatons, as

$$C(t) = \sum_{k,k'=1}^K \langle \hat{f}_k(t)\hat{f}_{k'}(0) \rangle_D = \sum_{k=1}^K c_k(t). \quad (2)$$

Here,  $\langle \hat{O} \rangle_D$  denotes the expectation value taken at the dissipaton vacuum state [56]. In this work, we adopt  $c_k(t) = \eta_k e^{-\gamma_k t}$ , lead to an exponential decomposition of  $C(t)$ , that can be accurately and routinely realized using the Prony decomposition algorithm. The resulting DD protocol is universal for arbitrary spectral density at any temperatures [57]. The exponents are either real or complex conjugate paired [55]. Therefore, we may determine  $\bar{k}$  by the pairwise equality  $\gamma_{\bar{k}} = \gamma_k^*$ . In the latter case, the dissipaton acquires both the characteristic energy and decaying rate, as the imaginary and real parts of  $\gamma_k$ , respectively. In the former case,  $\gamma_k$  is real ( $\bar{k} = k$ ) and the dissipaton mode purely decays.

The dissipaton is further second-quantized by the operator transformation

$$\hat{f}_k \xrightarrow{\text{SQ}} \zeta_k (\hat{b}_k^- + \hat{b}_k^+), \quad (3)$$

where  $\{\hat{b}_k^+\}$  and  $\{\hat{b}_k^-\}$  are bosonic creation and annihilation operators satisfying  $[\hat{b}_k^-, \hat{b}_{k'}^+] = \delta_{kk'}$ , with the choice of coefficient  $\zeta_k = \sqrt{(\eta_k + \eta_k^*)}/2$ . For each dissipaton, the Fock space  $\mathcal{H}_{f_k}$  is then generated, and one can thus establish the DQME-SQ for the dynamical variable  $\tilde{\rho}(t)$  of the extended system. Specifically,  $\tilde{\rho}(t)$  is represented as a density tensor in the reduced system space

$\mathcal{H}_S \otimes \mathcal{H}_S^*$  further dilated by the dissipaton Fock space  $\mathcal{H}_D = \otimes_k \mathcal{H}_{f_k}$ , i.e.,  $\tilde{\rho} \in \mathcal{H}_S \otimes \mathcal{H}_S^* \otimes \mathcal{H}_D$ . The constructed DQME-SQ reads

$$\begin{aligned} \dot{\tilde{\rho}}(t) = & -i[H_S, \tilde{\rho}] - \sum_k \gamma_k \hat{N}_k \tilde{\rho} \\ & - i \sum_k \zeta_k (\hat{b}_k^+ + \hat{b}_k^-) [\hat{Q}, \tilde{\rho}] + \sum_k \xi_k \hat{b}_k^+ \{\hat{Q}, \tilde{\rho}\}. \end{aligned} \quad (4)$$

Here,  $\{\cdot, \cdot\}$  denotes the anti-commutator,  $\hat{N}_k \equiv \hat{b}_k^+ \hat{b}_k^-$  and  $\xi_k \equiv (\eta_k - \eta_k^*)/2i\zeta_k$ . On the right-hand side of Eq. (4), the second term describes the decay of the dissipatons, and the last two terms account for the interactions between the system and the dissipatons. Compared with the pseudomode theory that utilizes a Lindblad equation in the space  $\mathcal{H}_S \otimes \mathcal{H}_S^* \otimes \mathcal{H}_D \otimes \mathcal{H}_D^*$  [21–23, 40, 41], Eq. (4) of the DQME-SQ theory is formulated in a more compact space, enabling more efficient numerical simulations.

For fermionic environments, the DQME-SQ theory can be established in a similar way. For a single-level system, we consider a common bilinear form of the system-environment coupling Hamiltonian,  $H_{SE} = \hat{c}^+ \hat{F}^- + \hat{F}^+ \hat{c}^-$ , which describes the exchange of fermionic particles between the system and environment. The DD for the environment hybridization operators reads

$$\hat{F}^\pm \xrightarrow{\text{DD}} \sum_{k=1}^K \hat{f}_k^\pm. \quad (5)$$

Here,  $\langle \hat{f}_k^\sigma(t) \hat{f}_{k'}^{\bar{\sigma}}(0) \rangle_D = \delta_{kk'} \eta_k^\sigma e^{-\gamma_k^\sigma t}$  with  $\sigma = \pm$  and  $\bar{\sigma} = -\sigma$ . Such a DD protocol completely recovers the environment correlation functions. The fermionic dissipaton Fock space is  $\mathcal{H}_D = \otimes_k (\mathcal{H}_{f_k^-} \otimes \mathcal{H}_{f_k^+})$ , which involves both the left and right actions of dissipaton creation and annihilation operators. Thus, the second quantization of fermionic dissipatons is realized through the following mappings.

$$\hat{f}_k^+ \hat{O} \xrightarrow{\text{SQ}} \zeta_k^+ \hat{b}_k^+ \hat{O} + \xi_k^- \hat{O} \hat{b}_k^+, \quad (6a)$$

$$\hat{O} \hat{f}_k^+ \xrightarrow{\text{SQ}} \zeta_k^+ \hat{b}_k^+ \hat{O} + \xi_k^{+*} \hat{O} \hat{b}_k^+, \quad (6b)$$

$$\hat{f}_k^- \hat{O} \xrightarrow{\text{SQ}} \zeta_k^- \hat{O} \hat{b}_k^- + \xi_k^+ \hat{b}_k^- \hat{O}, \quad (6c)$$

$$\hat{O} \hat{f}_k^- \xrightarrow{\text{SQ}} \zeta_k^- \hat{O} \hat{b}_k^- + \xi_k^{-*} \hat{b}_k^- \hat{O}, \quad (6d)$$

where  $\{\hat{b}_k^+\}$  and  $\{\hat{b}_k^-\}$  are fermionic creation and annihilation operators that satisfy  $\{\hat{b}_k^-, \hat{b}_{k'}^+\} = \delta_{kk'}$ , and the coefficients are chosen as  $\zeta_k^\sigma = (\eta_k^\sigma \eta_k^{\bar{\sigma}*})^{\frac{1}{4}}$  and  $\xi_k^\sigma = \eta_k^\sigma / \zeta_k^\sigma$ . The fermionic DQME-SQ reads

$$\begin{aligned} \dot{\tilde{\rho}} = & -i[H_S, \tilde{\rho}] - \sum_k (\gamma_k^- \hat{N}_k \tilde{\rho} + \gamma_k^+ \tilde{\rho} \hat{N}_k) \\ & - i \sum_k \left[ \zeta_k^- (\hat{c}^+ \hat{b}_k^- \tilde{\rho} - \hat{b}_k^- \tilde{\rho} \hat{c}^+) + \zeta_k^+ (\hat{c}^- \tilde{\rho} \hat{b}_k^+ - \tilde{\rho} \hat{b}_k^+ \hat{c}^-) \right. \\ & \left. + \xi_k^+ \hat{c}^+ \tilde{\rho} \hat{b}_k^- - \xi_k^{+*} \hat{b}_k^+ \tilde{\rho} \hat{c}^- - \xi_k^- \hat{c}^- \tilde{\rho} \hat{b}_k^+ + \xi_k^{-*} \tilde{\rho} \hat{b}_k^- \hat{c}^+ \right], \end{aligned} \quad (7)$$

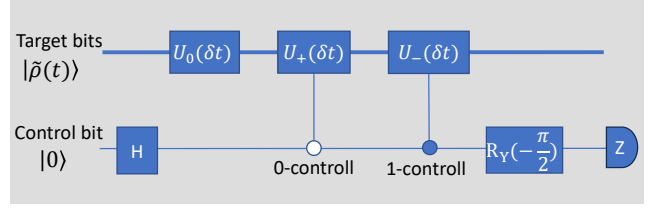


FIG. 2. Illustration of quantum circuit for the temporal propagation of DQME-SQ within a single time step by utilizing the LCU algorithm.

where  $\hat{N}_k \equiv \hat{b}_k^+ \hat{b}_k^-$  is the fermionic dissipaton number operator. Details on the analytic derivation are provided in Ref. [58]. The compactness of fermionic DQME-SQ theory is consistent with that of the bosonic case.

The DQME-SQ theory is in principle exact and universally applicable to both bosonic and fermionic environments, accommodating arbitrary spectral density and any temperature. Consistent with the HEOM theory, it captures the complete non-Markovianity. More importantly, the DQME-SQ offers a notable advantage: its formulation embraces a compact time-local structure within a minimized Hilbert space. This unique feature enables easy encoding into quantum circuits, distinguishing it from HEOM. While the computational complexity remains comparable to HEOM when implemented with classical algorithms, its excellent compatibility with quantum algorithms makes DQME-SQ a preferred choice for simulating complex non-Markovian OQS.

*Quantum simulation of DQME-SQ.* To simulate the non-Markovian open quantum dynamics governed by the DQME-SQ using quantum circuits, the first key step is encoding the extended density tensor. For both bosonic and fermionic environments, the extended density tensor  $\tilde{\rho}$  is mapped onto a pure qubit state,  $|\tilde{\rho}\rangle$ , as

$$|\tilde{\rho}\rangle \longmapsto |\tilde{\rho}\rangle = \frac{1}{C} \sum_{i, \mathbf{j}, \mathbf{n}} P_{ij}^{\mathbf{n}} |i\rangle \otimes |j\rangle \otimes |\mathbf{n}\rangle. \quad (8)$$

Here, the summation is over all the possible configurations of the extended system, where  $|\mathbf{n}\rangle = |n_1\rangle \otimes |n_2\rangle \cdots \otimes |n_K\rangle$  represents a dissipaton configuration. Note that for fermionic environments,  $|\mathbf{n}\rangle$  is formed by paired dissipaton Fock states. These configurations are encoded onto the qubits using a standard binary code. The global normalization coefficient  $C$  is determined by the probability conservation condition of  $\sum_i P_{ii}^{\mathbf{0}} = 1$ . The temporal evolution of  $|\tilde{\rho}(t)\rangle$  is then simulated by propagating the following equation of motion,

$$|\tilde{\rho}(t)\rangle = e^{-i\Lambda t} |\tilde{\rho}(0)\rangle, \quad (9)$$

where  $\Lambda$  is a non-Hermitian dynamical generator that represents the right-hand side of Eq. (4) or Eq. (7) [58].

The temporal propagation of  $|\tilde{\rho}(t)\rangle$  can be realized with various quantum algorithms, including the linear com-

combination of unitaries (LCU) [48, 59], quantum singular value transformation, time-dependent variational principle [47–49, 53], and others [41, 42]. Here, we utilize the LCU propagation [48]. Within a small time step  $\delta t$ , the propagator  $e^{-i\Lambda\delta t}$  is approximately decomposed as  $e^{-i\Lambda\delta t} = U_1(\delta t)U_0(\delta t)$ . Here,  $U_0(\delta t) \equiv e^{-i\Lambda_0\delta t}$  governed by a Hermitian generator,  $\Lambda_0 \equiv (\Lambda + \Lambda^\dagger)/2$ , is a unitary propagator, while  $U_1(\delta t) \equiv e^{-i\Lambda_1\delta t}$  governed by an anti-Hermitian generator,  $\Lambda_1 \equiv (\Lambda - \Lambda^\dagger)/2$ , is non-unitary. The latter is further approximated by

$$U_1(\delta t) \approx \frac{1}{2\epsilon}[U_+^\epsilon(\delta t) + U_-^\epsilon(\delta t)], \quad (10)$$

where  $U_\pm^\epsilon(\delta t) \equiv \pm i e^{\mp i\epsilon(I - i\Lambda_1\delta t)}$  is unitary and  $\epsilon$  is a real parameter that takes a sufficiently small value.

Shown in Fig. 2 is the designed quantum circuit of DQME-SQ comprising the target bits to store the density tensor state as well as a control bit for propagation. The input of the circuit is  $|\tilde{\rho}(t)\rangle \otimes |0\rangle$ . From the left to the right in the circuit, we first act a Hadamard gate (H) on the control bit, followed by the  $U_0(\delta t)$  gate on the target bits. Subsequently, the states go through the 0-control and 1-control gates of  $U_\pm^\epsilon(\delta t)$  successively. After acting an  $R_Y(-\pi/2)$  gate on the control bit, we obtain  $2\epsilon|\tilde{\rho}(t+\delta t)\rangle \otimes |0\rangle + |\text{unwanted}\rangle \otimes |1\rangle$ . Finally, by performing a Z-measurement on the control bit, we project out the unwanted state and obtain the target state  $|\tilde{\rho}(t+\delta t)\rangle$  with a probability depending on  $\epsilon$ . Once obtained, the wanted state will serve as the initial state for the next propagation step.

In contrast to classical algorithms whose computational costs grow exponentially as the system size or the complexity of non-Markovianity increases [14], the LCU algorithm exhibits highly favorable scalability – both the number of qubits and the circuit depth grow linearly with the increase of the number of dissipators. This favorable scalability makes the DQME-SQ theory, implemented with the LCU algorithm, as a promising approach to efficiently simulate complex non-Markovian open quantum dynamics.

*Numerical demonstrations.* We utilize the LCU algorithm to propagate the bosonic and fermionic DQME-SQ exemplified with spin-boson model and single-impurity Anderson model, respectively. To exhibit the feasibility of our framework, we employ the Aer simulator of Qiskit [60] to propagate the DQME-SQ. Within each time step, we directly extract the target state, bypassing the need for extensive probabilistic measurements required on actual quantum computing platforms.

The spin-boson model, with  $H_s = \Omega\hat{\sigma}_z + V\hat{\sigma}_x$ , is one of the most commonly used models that has broad applications in modern science. Here,  $\Omega$  and  $V$  are the energy difference and transfer coupling between two local states. On the other hand, the single-impurity Anderson model, with  $H_s = E_0(\hat{n}_\uparrow + \hat{n}_\downarrow) + U\hat{n}_\uparrow\hat{n}_\downarrow$ , is widely used in condensed matter physics to investigate the strongly cor-

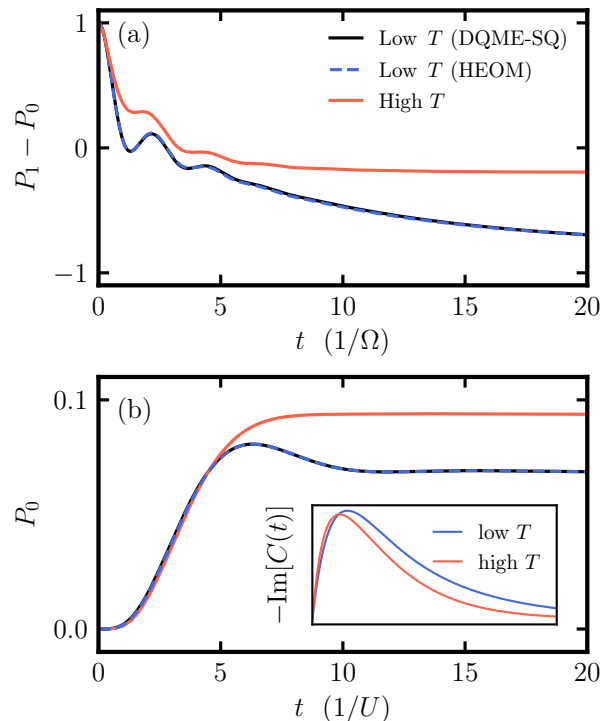


FIG. 3. (a) Simulated time evolution of  $P_1 - P_0$ , the population difference between two states, in a spin-boson theory, by using the quantum algorithm for the DQME-SQ compared to low and high temperature results via the classical propagation of HEOM; (b) Simulated time evolution of the ground-state population  $P_0$  for a single-impurity Anderson model, with inset depicting the imaginary part of the correlation function. Detailed parameters are provided in SM [58].

related transition metal impurities in metals. Here,  $E_0$  is the impurity level energy and  $U$  denotes the electron-electron interaction energy. For bosonic and fermionic environments, the non-Markovian memory associated with the temperature is manifested in the real and imaginary parts of the hybridization correlation function, respectively. In the fermionic case, as shown in the inset of Fig. 3(b),  $\text{Im}[C(t)]$  exhibits a longer extension in the time domain at lower temperatures. This indicates a more pronounced non-Markovian characteristics, which is anticipated to have a more significant impact on the dissipative dynamics of the system.

As shown in Fig. 3, the simulated time evolution results obtained from DQME-SQ and HEOM exhibit perfect agreement, where the HEOM method utilizes classical computation algorithms [58]. Notably, Fig. 3 demonstrates that non-Markovian effects are more pronounced at lower temperatures in both bosonic and fermionic environments. With all other parameters unchanged, a lower temperature leads to more pronounced oscillations in the short-time regime and slower relaxation in the long-time regime, due to longer environmental memory.

Due to limited computational resources at our dis-

posals, the digital quantum simulations presented above are constrained to minimal models. However, the utilized quantum algorithm will become universally feasible with significant advancements in future quantum computing technologies.

*Summary and perspective.* Towards the quantum simulation of non-Markovian open quantum dynamics, this paper presents the DQME-SQ theory, a universal and exact theory that enables quantum simulation of dissipative dynamics in both bosonic and fermionic environments. By translating the non-Markovian memory content into a compact description of statistical quasiparticles (dissipatons), the DQME-SQ theory provides a physical interpretation of OQS that is particularly suited for quantum computation, especially in fermionic environments. This framework provides extensive universality and flexibility for advancing quantum simulation in OQS, enhancing studies of nonequilibrium dynamics and thermodynamics by elucidating the roles of non-Markovian influences in complex OQS [61–64].

Support from the Ministry of Science and Technology of China (Grant No. 2021YFA1200103), the National Natural Science Foundation of China (Grant Nos. 21973086, 22103073, 22173088, 22373091, and 22393910), the Strategic Priority Research Program of Chinese Academy of Sciences (Grant No. XDB0450101), and the Fundamental Research Funds for the Central Universities (Grant No. WK2060000018) is gratefully acknowledged. The authors are indebted to Yu Su and Daochi Zhang for their invaluable help.

---

\* Authors of equal contributions

† wy2010@ustc.edu.cn

‡ xzheng@fudan.edu.cn

§ yanyj@ustc.edu.cn

- [1] U. Weiss, *Quantum Dissipative Systems*, World Scientific, Singapore, 2021, 5th edition.
- [2] H. P. Breuer and F. Petruccione, *The Theory of Open Quantum Systems*, Oxford University Press, New York, 2002.
- [3] H. Kleinert, *Path Integrals in Quantum Mechanics, Statistics, Polymer Physics, and Financial Markets*, World Scientific, Singapore, 5th edition, 2009.
- [4] A. Nitzan, *Chemical Dynamics in Condensed Phases: Relaxation, Transfer and Reactions in Condensed Molecular Systems*, Oxford University Press, New York, 2006.
- [5] B. J. Brown, D. Loss, J. K. Pachos, C. N. Self, and J. R. Wootton, *Rev. Mod. Phys.* **88**, 045005 (2016).
- [6] X. Zheng, Y. J. Yan, and M. Di Ventra, *Phys. Rev. Lett.* **111**, 086601 (2013).
- [7] H.-P. Breuer, E.-M. Laine, J. Piilo, and B. Vacchini, *Rev. Mod. Phys.* **88**, 021002 (2016).
- [8] I. de Vega and D. Alonso, *Rev. Mod. Phys.* **89**, 015001 (2017).
- [9] H. Lee, Y.-C. Cheng, and G. R. Fleming, *Science* **316**, 1462 (2007).
- [10] G. S. Engel, T. R. Calhoun, E. L. Read, T. K. Ahn, T. Mančal, Y. C. Cheng, R. E. Blankenship, and G. R. Fleming, *Nature* **446**, 782 (2007).
- [11] P. Nalbach, C. A. Mujica-Martinez, and M. Thorwart, *Phys. Rev. E* **91**, 022706 (2015).
- [12] S. Kundu, R. Dani, and N. Makri, *J. Chem. Phys.* **157**, 015101 (2022).
- [13] Y. Tanimura, *Phys. Rev. A* **41**, 6676 (1990).
- [14] Y. Tanimura, *J. Chem. Phys.* **153**, 020901 (2020).
- [15] Y. A. Yan, F. Yang, Y. Liu, and J. S. Shao, *Chem. Phys. Lett.* **395**, 216 (2004).
- [16] R. X. Xu and Y. J. Yan, *Phys. Rev. E* **75**, 031107 (2007).
- [17] J. S. Shao, *J. Chem. Phys.* **120**, 5053 (2004).
- [18] J. T. Stockburger and H. Grabert, *Phys. Rev. Lett.* **88**, 170407 (2002).
- [19] J. M. Moix and J. S. Cao, *J. Chem. Phys.* **139**, 134106 (2013).
- [20] L. Han, V. Chernyak, Y. A. Yan, X. Zheng, and Y. J. Yan, *Phys. Rev. Lett.* **123**, 050601 (2019).
- [21] D. Tamascelli, A. Smirne, S. F. Huelga, and M. B. Plenio, *Phys. Rev. Lett.* **120**, 030402 (2018).
- [22] D. Tamascelli, A. Smirne, J. Lim, S. F. Huelga, and M. B. Plenio, *Phys. Rev. Lett.* **123**, 090402 (2019).
- [23] N. Lambert, S. Ahmed, M. Cirio, and F. Nori, *Nature Comm.* **10**, 3721 (2019).
- [24] D. Suess, A. Eisfeld, and W. T. Strunz, *Phys. Rev. Lett.* **113**, 150403 (2014).
- [25] Y. Zhao, *J. Chem. Phys.* **158**, 080901 (2023).
- [26] Y. Ke, R. Borrelli, and M. Thoss, *J. Chem. Phys.* **156**, 194102 (2022).
- [27] M. Xu, Y. Yan, Q. Shi, J. Ankerhold, and J. T. Stockburger, *Phys. Rev. Lett.* **129**, 230601 (2022).
- [28] Y. L. Ke and Y. Zhao, *J. Chem. Phys.* **145**, 024101 (2016).
- [29] L. M. K. Vandersypen and I. L. Chuang, *Rev. Mod. Phys.* **76**, 1037 (2004).
- [30] T. D. Ladd, F. Jelezko, R. Laflamme, Y. Nakamura, C. Monroe, and J. L. O'Brien, *Nature* **464**, 45 (2010).
- [31] J. Biamonte, P. Wittek, N. Pancotti, P. Rebentrost, N. Wiebe, and S. Lloyd, *Nature* **549**, 195 (2017).
- [32] Y. Cao, J. Romero, J. P. Olson, M. Degroote, P. D. Johnson, M. Kieferova, I. D. Kivlichan, T. Menke, B. Peropadre, N. P. D. Sawaya, S. Sim, L. Veis, and A. Aspuru-Guzik, *Chem. Rev.* **119**, 10856 (2019).
- [33] S. McArdle, S. Endo, A. Aspuru-Guzik, S. C. Benjamin, and X. Yuan, *Rev. Mod. Phys.* **92**, 015003 (2020).
- [34] P. J. Ollitrault, G. Mazzola, and I. Tavernelli, *Phys. Rev. Lett.* **125**, 260511 (2020).
- [35] A. Miessen, P. J. Ollitrault, F. Tacchino, and I. Tavernelli, *Nat. Comput. Sci.* **3**, 25 (2023).
- [36] A. J. Daley, I. Bloch, C. Kokail, S. Flannigan, N. Pearson, M. Troyer, and P. Zoller, *Nature* **607**, 667 (2022).
- [37] R. Blatt and C. F. Roos, *Nat. Phys.* **8**, 277 (2012).
- [38] C. Gross and I. Bloch, *Science* **357**, 995 (2017).
- [39] H. Kamakari, S.-N. Sun, M. Motta, and A. J. Minnich, *PRX Quantum* **3**, 010320 (2022).
- [40] M. Cirio, S. Luo, P. Liang, F. Nori, and N. Lambert, *arXiv:2311.15240* (2023).
- [41] N. Lambert, M. Cirio, J. dong Lin, P. Mencil, P. Liang, and F. Nori, *arXiv:2310.12539* (2023).
- [42] S. Zhang, Y. Chen, and Q. Shi, *J. Chem. Phys.* **160**, 054101 (2024).
- [43] J. T. Barreiro, M. Müller, P. Schindler, D. Nigg, T. Monz, M. Chwalla, M. Hennrich, C. F. Roos, P. Zoller, and

- R. Blatt, *Nature* **470**, 486 (2011).
- [44] S. Barison, F. Vicentini, I. Cirac, and G. Carleo, *Phys. Rev. Res.* **4**, 043161 (2022).
- [45] X. Li and C. Wang, *Commun. Math. Phys.* **401**, 147 (2023).
- [46] J. Gacon, J. Nys, R. Rossi, S. Woerner, and G. Carleo, *Phys. Rev. Res.* **6**, 013143 (2024).
- [47] A. W. Schlimgen, K. Head-Marsden, L. M. Sager, P. Narang, and D. A. Mazziotti, *Phys. Rev. Lett.* **127**, 270503 (2021).
- [48] A. W. Schlimgen, K. Head-Marsden, L. M. Sager, P. Narang, and D. A. Mazziotti, *Phys. Rev. Res.* **4**, 023216 (2022).
- [49] K. Head-Marsden, S. Krastanov, D. A. Mazziotti, and P. Narang, *Phys. Rev. Res.* **3**, 013182 (2021).
- [50] M. S. Sarandy and D. A. Lidar, *Phys. Rev. Lett.* **95**, 250503 (2005).
- [51] S. Endo, J. Sun, Y. Li, S. C. Benjamin, and X. Yuan, *Phys. Rev. Lett.* **125**, 010501 (2020).
- [52] Y.-X. Yao, N. Gomes, F. Zhang, C.-Z. Wang, K.-M. Ho, T. Iadecola, and P. P. Orth, *PRX Quantum* **2**, 030307 (2021).
- [53] Y. Wang, E. Mulvihill, Z. Hu, N. Lyu, S. Shivpuje, Y. Liu, M. B. Soley, E. Geva, V. S. Batista, and S. Kais, *J. Chem. Theory Comput.* **19**, 4851 (2023).
- [54] X. Li, Y. Su, Z.-H. Chen, Y. Wang, R.-X. Xu, X. Zheng, and Y. Yan, *J. Chem. Phys.* **158**, 214110 (2023).
- [55] Y. J. Yan, *J. Chem. Phys.* **140**, 054105 (2014).
- [56] Y. Wang, Z. H. Chen, R. X. Xu, X. Zheng, and Y. J. Yan, *J. Chem. Phys.* **157**, 044102 (2022).
- [57] Z. H. Chen, Y. Wang, X. Zheng, R. X. Xu, and Y. J. Yan, *J. Chem. Phys.* **156**, 221102 (2022).
- [58] See Supplemental Material for detailed analytic derivations regarding the DQME-SQ theory and its numerical implementation.
- [59] L. Gui-Lu, *Commun. Theor. Phys.* **45**, 825 (2006).
- [60] Qiskit contributors, *Qiskit: An open-source framework for quantum computing*, 2023.
- [61] A. A. Clerk, M. H. Devoret, S. M. Girvin, F. Marquardt, and R. J. Schoelkopf, *Rev. Mod. Phys.* **82**, 1155 (2010).
- [62] A. Soare, H. Ball, D. Hayes, J. Sastrawan, M. C. Jarratt, J. J. McLoughlin, X. Zhen, T. J. Green, and M. J. Biercuk, *Nat. Phys.* **10**, 825 (2014).
- [63] G. Cohen, E. Gull, D. R. Reichman, and A. J. Millis, *Phys. Rev. Lett.* **115**, 266802 (2015).
- [64] R. Harper, S. T. Flammia, and J. J. Wallman, *Nat. Phys.* **16**, 1184 (2020).